

---

# Behaviour of pulsed vortex beam with high topological charge in ionized dielectrics

Khasanov<sup>1</sup> O.K., Fedotova<sup>1</sup> O.M., Smirnova<sup>1</sup> T.V., Petukh<sup>2</sup> Yu.N., Volyar<sup>3</sup> A.V. and Sukhorukov<sup>4</sup> A.P.

<sup>1</sup> Joint Institute of Solid State Physics and Semiconductors NAS,  
19 Brovki St., 220072 Minsk, Belarus

<sup>2</sup> Byelorussian State University, 4 Nezavisimosti Ave.,  
220050 Minsk, Belarus

<sup>3</sup> V.I. Vernadsky Taurida National University, 4 Vernadsky Ave.,  
95007 Simferopol, Ukraine

<sup>4</sup> Faculty of Physics, Moscow State University, 1  
Leninskie Gory, 119992 Moscow, Russia

Received: 23.11.2007

## Abstract

Dynamics of powerful femtosecond singular-phase pulsed beams in a dielectric medium is analyzed under the ionization conditions. The multiphoton ionization is revealed to contribute to the stable (quasi-soliton) regime of pulse propagation over the distances exceeding several diffraction lengths.

**Keywords:** femtosecond pulsed beam, singular phase, topological charge, Kerr nonlinearity, multiphoton ionization, free-electron plasma

**PACS:** 41.85.-p, 42.65.Jx

**UDC:** 535.31

## 1. Introduction

Up to date, a new field of physical optics has arisen, called as a singular optics [1–5]. Owing to their unique properties, singular-phase beams (SPB) are of particular interest for many applications. Among numerous examples, one should mention their use in optical tweezers or manipulating microparticles (the particles of sizes ranging from micro- to nano-scale, as well as those of biological tissues), including their cooling by optical trapping in a vortex field [6], and controlling the Bose-Einstein condensate [7]. While propagating, high-intensive SPB generate plasma, which has hollow-shaped form to yield waveguiding. Such a waveguide generated by the SPB is particularly advantageous for accelerating electrons [8] and subharmonic generation, including in the X-ray range [9]. Optical data storage, transmission and processing of information, quantum computers and quantum teleportation could also be reminded as possible applications [10].

A central problem in the theory and practice of the SPB, which is very important for the applications mentioned above, is their stability for the topological charge values  $m > 1$  in the linear and nonlinear propagation regimes. Until recently this problem has been addressed only in the framework of stationary or quasi-stationary interaction of beams with nonlinear media, although, according to M.S. Soskin and M.V. Vasnetsov [2], “it is time for the appearance of singular optics of ultrashort light pulses”.

Earlier it has been shown that the optical vortices are unstable in the media with self-focusing nonlinearity [11] and the vortex beams carrying a topological charge  $m$  split into  $2m$  filaments [12]. For comparison, vortex solitons can be stabilized in the media with defocusing cubic nonlinearity, as has been shown in [13]. Cubic-quintic model also demonstrates the conditions for stable propagation of tubular beams with  $m > 1$  [14–16], though the validity of this model has recently been under revision. In accordance with a number of works, vortex stabilization can be provided by nonlocal character of nonlinearity [17–19]. Particularly, the authors have discussed the existence and stability of two-dimensional solitons (single-charge vortex, dipole solitons and azimuthons) in the media with spatially nonlocal nonlinear response. Robustness of nonlocal solitons has been attributed to the fact that, by its nature, nonlocality acts as a sort of spatial averaging of the nonlinear response of the medium.

Apparently, inclusion of other defocusing factors, in particular, the effect of electron plasma due to multiphoton ionization (MPI) in the pulse field, would also promote stabilization of the pulsed beams that carry a vortex with a non-unit topological charge. As has been shown in [20], the balance between the Kerr self-focusing and the defocusing plasma effect can ensure waveguide propagation regime for the vortex-free (Gaussian) pulsed beams in the dielectric media, in particular in fused silica, through distances far exceeding the diffraction length. The conditions for this propagation depend on the ratio between the input beam power  $P_{in}$  and the critical power  $P_{cr}$  for self-focusing [20–21]. It should be noted that such the plasma formation has inertial character. Some temporal aspects of the nonlocality have been discussed in [20–21] (see also references therein).

In this work we study the propagation of tubular singular pulsed beams with different topological charges through a Kerr medium under the conditions of electron plasma formation due to MPI. We find the conditions for stable propagation of the beams under discussion. A comparative analysis is also made of free-electron generation in the field of vortex and non-vortex pulsed beams.

## 2. Mathematical model

Below we consider a situation close to the experimental one [22]: a light pulse with the wavelength  $\lambda = 800$  nm and the duration  $\tau_p = 70$ –100 fs passes through a fused silica sample. The input pulse intensity  $I_0$  varies in the 2–20 TW/cm<sup>2</sup> range. For these intensities of incident radiation it is expedient to investigate saturation of nonlinearity and photoionization of the medium. We analyze the propagation of doughnut-shaped hollow pulsed beam carrying the vortex with a topological charge  $m$  (Fig. 1).

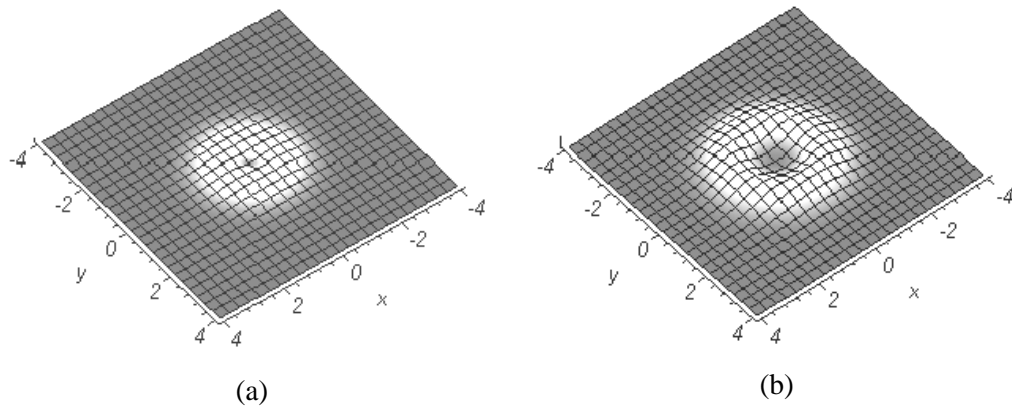


**Fig. 1.** Transverse structure of SPB field amplitude at the input for  $m=1$  (a) and  $m=3$  (b).

The pulse propagation through the medium is described by a set of equations represented in dimensionless form. It consists of the generalized nonlinear Schrödinger equation (1) for the complex envelope  $E = E(r', t', z')$  of the electric field under the assumptions of cylindrical symmetry, and the kinetic equation (2) for the free electron density  $\rho_e$  [23]:

$$\frac{\partial e}{\partial z} = iT^{-1} \left( \frac{\partial^2}{\partial r^2} + \frac{1}{r} \frac{\partial}{\partial r} \right) e - i \frac{L_{df}}{L_{ds}} \frac{\partial^2 e}{\partial t^2} + i \frac{L_{df}}{L_{nl}} T \left( |e|^2 - \kappa |e|^4 \right) - i \frac{L_{df}}{L_{pl}} \left( 1 - \frac{i}{\omega \tau_c} \right) \rho e - \left( \frac{L_{df}}{L_{mp}} |e|^{2(s-1)} + im^2 / r^2 \right) e, \quad (1)$$

$$\frac{\partial \rho}{\partial t} = |e|^{2s} - \rho \tau_p / \tau_r. \quad (2)$$

Here  $e = E(r', t', z') / E_0$  is the normalized field amplitude (i.e. the ratio of the field amplitude to that corresponding to the initial intensity  $I_0$  averaged over width),  $\rho = \rho_e / \rho_0$  the electron density normalized to its initial value  $\rho_0 = 10^9 \text{ cm}^{-3}$ ,  $L_{df} = kw_0^2 / 2$  the diffraction length (with  $w_0$  being the initial beam radius and varying in the range of 10-70  $\mu\text{m}$ ),  $L_{ds} = \tau_p^2 / \beta_2$  the dispersion length ( $\beta_2 = 361 \text{ fs}^2/\text{cm}$  being the group velocity dispersion, abbreviated as GVD further on),  $L_{nl} = c / \omega n_2 I_0$  the nonlinear length,  $I_0 = n_0 c |E_0|^2 / 2\pi$  denotes the peak input intensity,  $n_0$  ( $n_2$ ) the linear (nonlinear) refractive index for the quartz glass ( $n_2 = 3 \times 10^{-16} \text{ cm}^2/\text{W}$ ),  $L_{pl} = 2\rho_0 / \sigma \omega \tau_c$  the plasma absorption length (with  $\sigma = 1.55 \times 10^{-18} \text{ cm}^2$  being the cross section for the inverse bremsstrahlung and  $\tau_c = 2.33 \times 10^{-14} \text{ s}$  the electron collision time), and  $L_{mp} = 1 / \beta^{(s)} I_0^{s-1}$  is the  $s$ -photon absorption length with the coefficient  $\beta^{(s)}$ , where  $s$  implies the number of photons in the

multiphoton absorption (MPA) process ( $s = 6$  for the fused silica). Regarding the rest of the notation,  $\kappa = n_4 / n_2 I_0^2$  represents the saturation parameter,  $m = \pm 1, \pm 2, \dots$  the topological charge, and  $\tau_r$  the electron recombination time resulting from electron-phonon interaction ( $\tau_r = 300 \times 10^{-15}$  s). The dimensionless variables are  $z = z' / L_{df}$ ,  $r = r' / w_0$  and  $t = (t' - z' / v_{gr}) / \tau_p$ , where  $z$  and  $r$  are the dimensionless longitudinal and lateral variables and  $t$  the dimensionless time in the frame of reference moving with the velocity  $v_{gr}$ . All the coefficients entering Eqs. (1) and (2) are real and expressed in terms of the physical parameters of the problem.

In the above system, the terms on the r. h. s. of Eq. (1) describe the mechanisms of diffraction, group velocity dispersion, cubic and quintic nonlinearities, plasma defocusing and MPA for dielectrics. The operator  $T \equiv 1 + i \frac{\partial}{\partial t} \frac{1}{\omega \tau_p}$  in Eq. (1) characterizes the measure of departure from the approximation of slowly varying envelope. It introduces a correction arising from the effects of spatiotemporal focusing and increase in the envelope steepness.

In the kinetic equation for the free-electron density, the first term on the r. h. s. describes the MPI and the second accounts for the electron recombination. Provided that the duration of the propagating pulse is far shorter than the electron-phonon relaxation time, the effect of recombination can be neglected in the subsequent discussion.

The boundary conditions for the field amplitude at  $z=0$  are chosen as follows:

$$e(z=0) = e_0 \frac{|r|^m}{m^2} \exp(-r^2 / 2m^2 - t^2 / 2); \quad \partial e / \partial r|_{r=0} = e_{r=R} = 0. \quad (3)$$

Here  $e_0 = E_0^* / E_0$  (with  $E_0^*$  being the peak field amplitude at the input) and  $R$  meets the condition  $e_{r>R} = 0$  for all  $z \in [0, L]$ , where  $L$  is the dimensionless length of the sample.

### 3. Conservation laws

It is well known that the conservation laws play an important part in the studies of in-medium radiation waveguide propagation regimes. Consider the propagation equation (1) for the field  $e$  without the components caused by the operator  $T$ :

$$\frac{\partial e}{\partial z} = i\Delta_{\perp} e - i\delta \frac{\partial^2 e}{\partial \tau^2} + ic_3 |e|^2 e - ic_5 |e|^4 e - \gamma(1 + i\omega_0 \tau) e - \mu_s |e|^{2s-2} e - i \frac{m^2}{r^2} e, \quad (4)$$

where  $c_3 = \frac{8P_{in}}{P_{cr}}$ ,  $c_5 = \kappa$ ,  $P_{in} = \frac{w_0^2 n_0 c |E_0|^2}{2}$ ,  $P_{cr} = \frac{\lambda_0^2}{2\pi n_0 n_2}$ ,  $\delta = \frac{k w_0^2 \beta_2}{4 \tau_p^2}$  and

$\mu_s = \frac{k w_0^2}{4} \beta^{(s)} \left| \frac{2^{m+1} P_{in}}{\pi m! w_0^2} \right|^{s-1}$ . In the absence of dissipation it is easy to show that the Hamiltonian of the problem  $H$  is as follows:

$$H = \int \int_{\tau \bar{r}_\perp} \left( |\nabla_\perp e|^2 - \delta \left| \frac{\partial e}{\partial \tau} \right|^2 - \frac{c_3}{2} |e|^4 + \frac{c_5}{3} |e|^6 + \frac{m^2}{r^2} |e|^2 \right) d\bar{r}_\perp d\tau. \quad (5)$$

Moreover, Eq. (1) is characterized by another integral of motion, which implies the energy conservation law. The total wave power is conserved in the absence of dissipation:

$$P(z) \equiv \int \int_{\tau \bar{r}_\perp} |e|^2 d\bar{r}_\perp d\tau. \quad (6)$$

Suppose that the field envelope at the sample input  $z=0$  has the form

$$e(\bar{r}_\perp, \tau, z=0) = e(r_\perp, \varphi, \tau, z=0) = \frac{w_f}{w_0} r^m \exp \left( -\frac{w_f^2}{w_0^2} r_\perp^2 - \frac{\tau^2}{\tau_p^2} - ik_0 \frac{w_f^2}{2f} r_\perp^2 + im\varphi \right), \quad (7)$$

where  $f$  is the focus distance,  $w_f$  the beam radius at the focus and  $w_0$  the input beam radius.

Note that the transverse and temporal mean-square radii are very important characteristics of the pulsed light beams propagating through a bulk medium. They are as follows:

$$\bar{R}^2(z) \equiv \frac{1}{P(z)} \int \int_{\tau \bar{r}_\perp} |r_\perp - \langle \bar{r}_\perp(z) \rangle|^2 |e|^2 d\bar{r}_\perp d\tau, \quad (8)$$

$$\bar{T}^2(z) \equiv \frac{1}{P(z)} \int \int_{\tau \bar{r}_\perp} |\tau - \langle \tau(z) \rangle|^2 |e|^2 d\bar{r}_\perp d\tau. \quad (9)$$

Here  $\langle \bar{r}_\perp(z) \rangle \equiv \frac{1}{P(z)} \int \int_{\tau \bar{r}_\perp} r_\perp |e|^2 d\bar{r}_\perp d\tau$  and  $\langle \tau(z) \rangle \equiv \frac{1}{P(z)} \int \int_{\tau \bar{r}_\perp} \tau |e|^2 d\bar{r}_\perp d\tau$  are the trans-

verse and temporal centres of mass of the pulsed beam, respectively. We have obtained these characteristics for the SPB by substituting their shape given by Eq. (7) into Eqs. (5), (6), (8), (9) and (4). Omitting any intermediate calculations, we will present only the final expressions for the integrals of motion. Below we consider the case when the pulse duration  $\tau_p$  is such that the GVD weakly affects the pulse dynamics. Then the Hamiltonian of the problem in the moving reference frame may be written as

$$H = \frac{1}{2^m} \left( \frac{\pi}{2} \right)^{\frac{3}{2}} \left( \frac{w_0^2}{w_f^2} \right)^{m-1} \left[ \left( 3 - 2 \left( 1 + \frac{z_0}{f} \right) \right) mm! + \left( 1 + \frac{z_0^2}{f^2} \right) (m+1)! - \frac{c_3 \sqrt{2}}{2^{3m+4}} \left( \frac{w_0^2}{w_f^2} \right)^m (2m)! \right], \quad (10)$$

where  $z_0$  is the diffraction length and  $z_f$  the Rayleigh length. As for Eq. (6), we get

$$P_\perp = \left( \frac{\pi}{2} \right)^{\frac{3}{2}} \frac{1}{2^{m+1}} \left( \frac{w_0^2}{w_f^2} \right)^m m!. \quad (11)$$

As expected earlier, the total energy of the singular pulse depends upon its topological charge and increases strongly with increasing  $m$ .

In general, in order to get introductory information on the SPB behaviour it would be enough to obtain the expression for the mean-square radius. But this task is very cumbersome. Fortunately, it has been ascertained that the second derivative of  $\langle R^2 \rangle$  is  $d_z^2 \bar{R}^2(z) = \frac{8H}{P_\perp}$ , what is the same as for the case of Gaussian beams [20]. Therefore, we get the sought function  $\bar{R}^2(z)$  after integrating twice the expression for  $d_z^2 \bar{R}^2(z)$ . The final expression for the dimensionless transverse mean-square radius of the SPB bearing the topological charge  $m$  in the Kerr medium takes the form

$$\bar{R}^2(z) = \frac{8z_f}{z_o} \left[ \left[ 3 - 2 \left( 1 + \frac{z_0}{f} \right) \right] m + \left( 1 + \frac{z_0^2}{f^2} \right) (m+1) - \frac{c_3 \sqrt{2}}{2^{3m+4}} \left( \frac{z_f}{z_o} \right)^m \frac{(2m)!}{m!} \right] z^2 + \left( 2m - \frac{k_0 w_0^2}{f} \right) (m+1) z + \frac{m+1}{2} \frac{z_0}{z_f} \quad (12)$$

This is valid for the case of minimal dissipation losses and negligible plasma contribution. It is worth mentioning that all the expressions obtained by us at  $m=0$  coincide with those presented in the work [20] for the Gaussian beam.

Note that Eq. (12) allows one to describe dynamics of the radiation in the medium. As one can conclude, the mean-square radius of the beam changes during its propagation. It can increase or decrease, depending on the corresponding parameters and thus resulting in self-focusing or defocusing. Moreover, the self-focusing and defocusing stages would periodically alternate. In other words, a refocusing regime of tubular pulse propagation in the medium may be expected under certain conditions. A more detailed analysis based on numerical solution of the system mentioned above is presented below.

#### 4. Numerical simulation technique

Detailed information on the nonlinear dynamics of the SPB in the Kerr medium under photoinduced ionization conditions as a function of their topological charge can be got by means of modelling the propagation process numerically. For this aim we have solved the set of Eqs. (1) and (2) with the boundary conditions given by Eq. (3) in the domain  $D = [0 \times R] \times [0, L] \times [-T, T]$  (with  $T$  being the characteristic time) by introducing a mesh uniform in  $t$  and nonuniform in  $r$  and  $z$ , which becomes finer in the region of strong gradients. On this mesh, the initial problem has been approximated by a system of difference equations and solved on the basis of iterative alternating direction method [24].

The system of equations with three-diagonal matrices has been solved using the sweep technique combined with iterations, while the electron density equation has been integrated with the Runge-Kutta method. In the region of strong spatial gradients, we have made use of steps variable in the  $z'$  coordinate.

Nonuniform approximate mesh construction has been used in Ref. [25] in the investigation of pulse filamentation in the air, which has allowed optimizing substantially the simulation procedure and attaining high precision. The construction algorithm we employ implies the use of a step in the coordinate  $r'$ , which varies according to geometric series law. The geometric ratio is  $q = \left[ (1 + \varepsilon / N_r)^{N_r} - 1 \right] / \varepsilon$ , with  $N_r$  being the number of steps and  $\varepsilon \ll N_r$  if the mesh is refined in the paraxial region. To provide conservatism of the constructed difference scheme, the balance method has been used.

## 5. Results of numerical analysis

Numerical simulations were performed for the following input parameters of the pulsed beams. The ratio  $P_{in}/P_{cr}$  was changed from 1.5 to 20 ( $P_{cr} = 0.159 \cdot \lambda_0^2 / (n_0 n_2) \sim 2.2$  MW). The initial beam radius  $w_0$  was varied in the 10-25  $\mu\text{m}$  range. The diffraction length  $L_{df}$  of the beam with  $w_0 = 10$   $\mu\text{m}$  was equal to 0.57 mm. For the initial intensities employed the nonlinear length was  $L_{nl} \ll L$ . The dispersion length  $L_{ds}$  exceeded  $L_{df}$  by three orders of magnitude for  $\tau_p = 100$  fs, the plasma length was  $L_{pl} \sim 10^6$  m and  $L_{mp} \sim 10^2$  m.

Numerical experiment has demonstrated the existence of radial compression and spreading stages in the pulse evolution in the medium. As the beam propagates, there occurs a beam compression at the first stage, which is due to dominating contribution of focusing cubic nonlinearity to the field intensity. Fig. 2 shows radial distribution of the peak intensity of the pulse with the topological charge  $m = 2$  at the stage of compression,

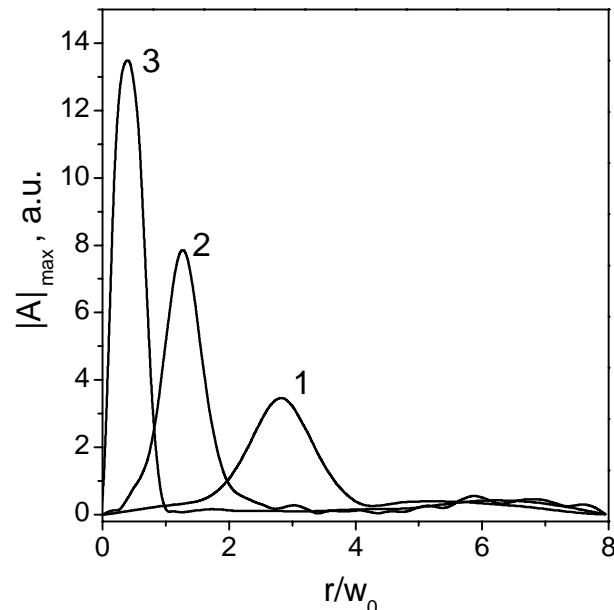


**Fig. 2.** Transverse distribution of singular pulse amplitude for the initial values  $\tau_p=100$  fs,  $I_0=2$  TW/cm<sup>2</sup>,  $w_0=10$   $\mu\text{m}$ ,  $m=2$  and at different  $z$  values: (1)  $z=0.2L_{df}$ , (2)  $z=0.7L_{df}$  and (3)  $z=1.1L_{df}$ .

when the beam radius shrinks to 1/3 of its initial value and the intensity increases. With increasing intensity the effect of defocusing related to the fifth-order nonlinearity and plasma increases, too. The spreading stage is primarily attributable to the effect of defocusing.

It has been found that these structural changes of the pulsed beam manifest a clearly defined periodicity as the beam propagates along the  $z'$  axis (see Fig. 3). The maximum amplitude increases and the pulse narrows down until the effect of defocusing nonlinearities, which becomes stronger with increasing intensity, terminates its further increase. In this case, the beam aperture becomes smaller. In other terms, a multiple self-focusing of the beam is observed. With increasing saturation parameter (i.e., an increase in  $n_4$  or  $I_0$ ), the oscillation periods of the beam intensity and its aperture become shorter. When the generated plasma is not a dominant defocusing factor (the estimates of the contributions of nonlinearity-related terms in Eq. (1) show that this takes place for  $P/P_{cr} \sim 1.5$ ) and exerts only additional defocusing effect, it limits growth of the intensity and shortens period of its oscillations. As the beam propagates, the energy dissipation due to multiphoton and plasma absorptions gives rise to lowering beam intensity and increasing period of its oscillations. We mark that the effect of group delay dispersion is insignificant in the case under consideration, which is also confirmed by the numerical analysis.

When the plasma plays a dominant part in defocusing (the radiation power localized in the transmitted beam exceeds the incident radiation power by an order of magnitude), the periodicity exhibits features arising from the inertial character of plasma formation.

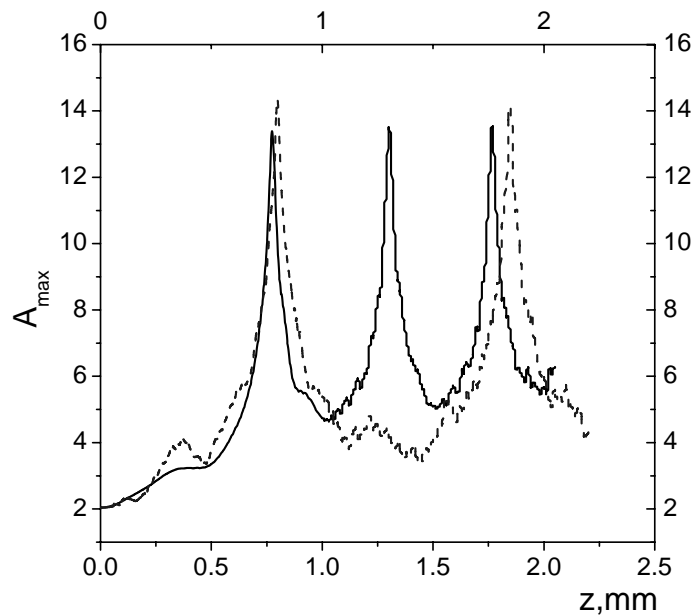


**Fig. 3.** Multifoci behaviour of SPB at the maximum field amplitude,  $I_0=2.25 \text{ TW/cm}^2$ ,  $w_0=20 \text{ }\mu\text{m}$ ,  $\tau_p=100 \text{ fs}$  and the propagation in case of different  $m$  values:  $m=2$  (solid line) and  $m=3$  (dashed line).



One might expect that the periodical beam behaviour would also change. This has been observed experimentally in Ref. [26]. Our simulations ( $m \neq 0$ ) have shown that the periodicity is violated when the defocusing effects of plasma and fifth-order nonlinearity are comparable in magnitude (for  $P_{in}/P_{cr} \sim 5$ ).

It has turned out that the use of the SPB enables substantial increase in the free-electron plasma density, when compare with the case of Gaussian pulses, due to rise in the laser radiation intensity, coming from the very structure of electron density distribution in the radiation propagation through the sample as a function of the topological charge. Our numerical calculations show that when the input intensity  $I_0$  is varied in the 2-9 TW/cm<sup>2</sup> range, the free-electron density increases by a factor of 3–5, compared to the case of ordinary (non-singular) Gaussian beams [27] (see Fig. 4 and the corresponding insert). The density distribution is determined by the transverse beam profile, in particular by increase in its slope occurring when the topological charge increases. Then the dip in the intensity distribution broadens at the centre of the tubular beam and its 'walls' become thinner. The higher the topological charge, the smaller is the volume occupied by the field. This leads to increase in the field density and the density of free electrons, the other parameters remaining the same. Further density increase is still possible for the beams with higher topological charges (Fig. 5). Then the increase in the plasma density quickens with increasing input radiation intensity, and the free-electron density peak is observed to shift towards shorter distances in the sample.

In other words, the plasma density may reach critical values in the field of high-power SPB. The use of these beams may therefore turn out to be preferable when generating higher-order harmonics, electrons and X-ray radiation in the pulsed regime.

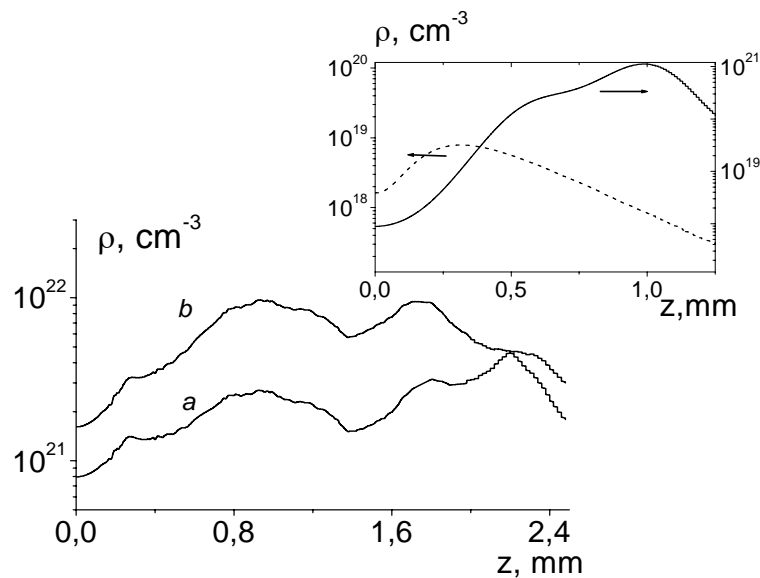


**Fig. 4.** Average electron density vs propagation distance for vortex pulses:  $t_p = 100$  fs;  $w_0 = 10$   $\mu\text{m}$ ,  $m = 2$ ,  $I_0 = 2$  TW/cm<sup>2</sup> (a) and  $I_0 = 2.8$  TW/cm<sup>2</sup> (b). Insert: electron density for Gaussian ( $m = 0$ ) and vortex ( $m = 2$ ) pulse

As follows from Fig. 5, the electron plasma density achieves too high value for the high  $m$  values ( $m \geq 3$ ). Apparently, modifying the model under analysis and including properly the radiative recombination processes would be worth considering.

We emphasize that the fifth-order nonlinearity is nothing more than the first approximation in the inclusion of nonlinearity saturation in the field of high-power pulses and its role in the stabilisation of vortex solitons has not been studied. At the same time, the generated plasma can do more than merely play a significant defocusing part. The very plasma production process is actually responsible for a nonlocal character of the light-matter interaction, and this may be the main factor when attaining the vortex beam stability condition, similar to the other types of nonlocal nonlinearities (the thermal nonlinearity [18] and the spatial dispersion [28]).

## 6. Conclusions

We have investigated for the first time the evolution, in a dielectric medium, of high-power pulsed femtosecond vortex beams bearing different topological charges  $m$ , using the example of quartz glass under optically induced ionization conditions. As a model, we have employed a system consisting of the modified  $(2 + 1)$ -dimensional nonlinear Schrödinger equation and the kinetic equation for the free-electron density. The main simulation results and conclusions may be formulated as follows:

When a pulsed vortex beam with a near-critical input power propagates through a nonlinear dielectric medium under the conditions of weak dissipation and dispersion effects, the competition of focusing and defocusing factors has the effect that the beam structure behaves in a periodic manner along the propagation axis. In this case, the effect of plasma is an auxiliary factor. With increasing input beam power, the defocusing factors related to the plasma and the fifth-order nonlinearity become comparable in their magni-

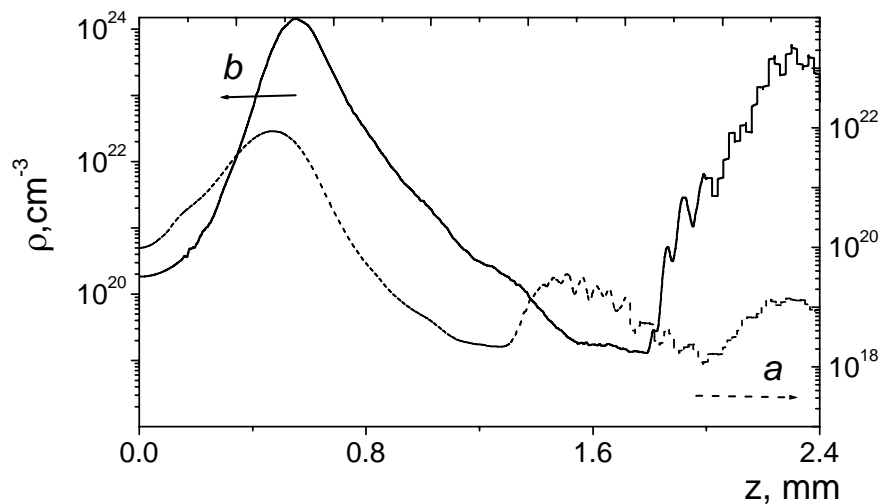


**Fig. 5.** The same as in Fig. 4, for the parameters  $\tau_p = 100$  fs,  $w_0 = 10$   $\mu\text{m}$ ,  $I_0 = 3$  TW/cm<sup>2</sup>,  $m=2$  (a) and  $m=3$  (b).

tude and bring about a violation of the above periodicity. Since the beam retains its shape, it would be correct to say that it propagates in a quasi-soliton regime.

The interaction of the SPB with the nonlinear ionizable dielectric medium under study permits attaining higher light field densities and generating higher plasma densities, when compare with the ordinary (non-singular) pulsed beams. The plasma density increases with increasing topological charge of the vortex beam.

The analysis of nonlinear dynamics of beams possessing orbital angular momentum, with the inclusion of contributions from the competing processes, calls for a more detailed investigation. In particular, it would be of interest to elucidate the role of (normal or anomalous) group velocity dispersion, the increase in the beam profile slope and the spatiotemporal beam focusing. We intend to analyze these points in the course of further investigations.

## References

1. Nye, JF and Berry MV, 1974. Dislocations in wave trains. Proc. Roy. Soc. London, Ser.A **336**: 165-190.
2. Soskin MS and Vasnetsov MV, 2001. *Singular optics*, In: Progress in Optics, Ed. E. Wolf (North-Holland, Amsterdam), **42**: 219-276.
3. Vasnetsov M.V., Staliunas K., Optical Vortices (Horizons in World Physics 228), Commack, New York: Nova Science Publishers, 1999.
4. Allen L, Padgett MJ, Babiker M, 1999. The orbital angular momentum of light. In: Progress in Optics (North-Holland, Amsterdam) **39**: 291-372.
5. Yin J, Gao W, Zhu Y, 2003. Generation of dark hollow beams and their applications. In: Progress in Optics, North-Holland, Amsterdam **45**: 119- 204.
6. Ashkin A, Dziedzic JM, Bjorkholm JH and Chu S, 1986. Observation of a single-beam gradient force optical trap for dielectric particles. Opt. Lett. **11**: 288-290.
7. Bongs K, Burger S, Dettmer S, Hellweg D, Arlt J, Ertmer W, Sengstock K, 2001. Waveguide for Bose-Einstein Condensates. Phys. Rev. **A63**: 031602/1-4.
8. Esarey E, Sprangle P, Krall J and Ting A, 1996. Overview of plasma-based accelerator concepts. IEEE Trans. Plasma Sci. **24**: 252-288.
9. Milchberg HM, Durfee CC, McIlrath TJ, 1995. High-order frequency conversion in the plasma waveguide. Phys. Rev.Let. **25**: 2494-2497.
10. Muthukrishnan A, Stroud Jr CR, 2002. Entanglement of internal and external angular momenta of a single atom. J. Opt. B. **4**: S73-S77
11. Kivshar Yu.S., Agrawal G.P., Optical solitons: from fibers to photonic crystals. San Diego: Academic Press, (2003).
12. Bigelow MS, Zerom P, Boyd RW, 2004. Breakup of Ring Beams Carrying Orbital Angular Momentum in Sodium Vapor. Phys. Rev.Let. **92**: 083902/1-3.
13. Desyatnikov AS, Kivshar YuS, and Torner L, 2005. Optical vortices and vortex solitons, in Progress in Optics. Ed. E. Wolf (Elsevier, Amstredam) **47**: 219-319.

14. Desyatnikov A, Maimistov A, Malomed B, 2000. Three-dimensional spinning solitons in dispersive media with the cubic- quintic nonlinearity. *Phys. Rev. E* **61**: 3107-3113.
15. Towers I, Buryak A, Sammut R, Malomed B, Crasovan L, and Mihalache D, 2001. Stability of spinning ring solitons in the cubic-quintic nonlinear Schroedinger equation. *Phys. Rev. A* **288**: 292-298.
16. Kartashov YV, Carretero-González R, Malomed BA, Vysloukh VA, and Torner L, 2006. Multipole-mode solitons in Bessel optical lattices. *Optics Express* **26**: 10703-10710.
17. Skupin S., Saffman M., Krolikowski W., Bang O., 2007. Enhanced stability of nonlocal solitons in saturable focusing media. *CLEO®/Europe-IQEC'2007*, Munich, Germany: CD1-2-MON.
18. Skupin S, Bang O, Edmundson D, and Krolikowski W, 2006. Stability of two-dimensional spatial solitons in nonlocal nonlinear media. *Phys. Rev. E* **73**: 066603/1-8.
19. Buccoliero D, Lopez-Aguayo S, Skupin S, Desyatnikov AS, Bang O, Krolikowski W, Kivshar YS, 2007. Spiralling solitons and multipole localized modes in nonlocal nonlinear media. *Physica B* **394**: 351–356.
20. Berge L, Couairon A, 2000. Nonlinear propagation of self-guided ultra-short pulses in ionized gases. *Physics of Plasmas*. **7**: 210-230.
21. Tzortzakis S, Sudrie L, Franco M, Prade B, Mysyrowics A, Couairon A, Berge L, 2001. Self-guided propagation of ultrashort IR laser pulses in fused silica. *Phys. Rev. Lett.* **87**: 213902/1-4.
22. Von der Linde D, Schuler HJ, 1996. Breakdown Threshold and Plasma Formation in Femtosecond Laser-Solid Interaction. *J. Opt. Soc. Am. B* **13**: 216-222.
23. Gaeta A, 2000. Catastrophic collapse of ultrashort pulses. *Phys.Rev.Lett.* **84**: 3582-3585.
24. Samarskii A.A. The theory of difference schemes. Moscow: Nauka, (1989).
25. Kandidov VP, Kosareva OG, Koltun AA, 2003. Nonlinear-optical transformation of a high-power femtosecond laser pulse in air. *Quant. Elektr.* **33**:69-75.
26. Wu Zh, Jiang H, Luo L, Guo H, Yang H, and Gong Q, 2002. Multiple foci and a long filament observed with focused femtosecond pulse propagation in fused silica *Opt. Lett.* **27**: 448-450.
27. Khasanov OK, Smirnova TV, Fedotova OM, Suhorukov AP, von der Linde D, 2003. Powerful femtosecond pulse interaction with Kerr dielectrics. In *Jubil. Digest: "Topical problems of solid state physics"* Minsk, Belorusskaya Navuka: 573-583.
28. Turitsyn SK, 1997. Theory of an average pulse propagation in high-bit-rate optical transmission systems with strong dispersion management. *JETP Letters*. **65**: 812-817.